Materials Research. 2023; 26:e20230225
DOI: https://doi.org/10.1590/1980-5373-MR-2023-0225

Wear Behaviour Analysis of Heat Treated A356 Composite with Copper and Copper-Coated Zinc as Reinforcements

K. Nithesh[a], *Sharma Sathyashankara*[a]*, *Nayak Rajesh*[a], *M.C. GowriShankar*[a], *B.M. Karthik*[a], *Srinivas Doddapaneni*[a]

[a]*Manipal Academy of Higher Education, Manipal Institute of Technology, Department of Mechanical and Industrial Engineering, 576104, Manipal, India.*

Received: May 05, 2023; Revised: August 17, 2023; Accepted: September 14, 2023

The present study reflects on the wear behaviour characteristics of A356 composite with trace addition of copper and copper-coated zinc as reinforcements. Dry sliding wear tests were conducted on fabricated as-cast and heat treated composites by varying load of 20-60 N under constant sliding speed of 1 m/s and sliding distance of 3000 m. Results confirmed that copper-coated zinc was successfully introduced as reinforcement into A356 matrix using two-step casting method. Scanning Electron Microscope (SEM) images confirmed the presence and homogeneous distribution of the added reinforcements in the matrix. T6 treatment with addition of Cu reinforcement facilitated age hardening showing 121% hardness improvement compared to as-cast matrix A356. At lower loads, wear results showed 117-134% enhanced wear resistance in composite reinforced with 1 wt.% Cu and aging at 100°C. However at higher loads, 153-210% improvement in wear resistance was observed. Overall, copper and Cu-coated zinc reinforced composite along with T6 treatment exhibited significant improvement in hardness wear property compared to as-cast matrix A356 alloy.

Keywords: *A356 alloy, Aluminum Matrix Composite (AMC), Age hardening, Copper-coated zinc reinforcements.*

1. Introduction

Aluminum alloys have gained significant popularity across various industries in recent times due to their exceptional characteristics, such as lightweight, high strength-to-weight ratio, good conductivity, malleability, high heat conductivity, and excellent corrosion resistance[1-3]. The aerospace and automotive industries find aluminum alloys to be a desirable option for numerous applications because of their lightweight nature, which is crucial for ensuring durable structures[4,5]. The popularity of aluminum alloys is expected to continue to grow as more industries discover their many benefits and as new manufacturing processes are developed to make them even more cost-effective and sustainable. The addition of reinforcement elements like copper, silicon, and magnesium, along with suitable heat treatment are known to enhance the wear resistance property of aluminum alloys[6-10]. Incorporating silicon as hypoeutectic alloying element enhances its mechanical and wear properties, reaching the optimum level at its eutectic composition, typically around 12% silicon in aluminum-silicon alloys[11]. Above this composition, the excess silicon can have a negative impact on the properties, leading to reduced ductility and increased brittleness[12].

Aluminum-silicon (Al-Si) A356 alloys are one of the widely used material in industrial applications, which is a hypoeutectic alloy containing around 7 to 9% silicon. Furthermore, addition of reinforcements can help to tailor the properties of A356 alloy, so as to meet the requirements of specific applications, resulting in a high-performance material with improved properties and performance characteristics[13,14]. The addition of copper to A356 can lead to improvements in the strength, stiffness, wear resistance, and thermal stability of the alloy[15,16]. The copper reinforcement can also help to improve the fatigue life of the alloy, making it more resistant to failure due to cyclic loading. In addition, zinc is also introduced as reinforcement in minor quantity to study the change in property. To avoid the dissolution of lower melting point zinc in the matrix during processing, a copper coating with a high melting point was employed[17-19]. By utilizing this approach in combination with suitable heat treatment, it is possible to control the development of high strength and hard copper-zinc intermetallics[20]. A356 alloys are mainly used in tribocomponents for sliding movement with a counterbody. Their performance depends on material parameters and service conditions, which affect wear behavior. Even minor parameter changes can significantly impact wear behavior. Therefore, comprehensive characterization of mechanical properties and sliding wear behavior is crucial for understanding their performance in different situations[21-23]. T6 artificial aging is one of the heat treat process generally used to impart high strength in A356 cast alloys by solutionizing and quenching the material, then aging at a high temperature to break down the solid solution into a more stable and finely dispersed precipitate structure resulting in enhanced strength and ductility[24-27].

*e-mail: ss.sharma@manipal.edu

A number of studies on wear behaviour of Al-Si alloys have been reported previously. However, only a limited number of articles have focused on investigating effect of reinforcement addition on enhancement of wear and friction properties in Al-Si alloys. Hassan et al.[28] found that adding SiC reinforcement particles improved wear resistance property in Al-Mg-Cu composite than pure aluminium alloys. The rate of wear volume loss was found to be significantly lower in composite samples. Wear resistance property increased up to 5 wt.% Cu addition but had no substantial influence on friction coefficient values. In their study, Alias and Haque[29] showed significant parameters as applied load and sliding distance effecting wear in Al-Si eutectic alloys. In addition, T6 treatment effectively contributed in enhanced wear resistance property due to inherent properties defined by the matrix. Sudarshan and Surappa[30] conducted a study to analyze the sliding wear behaviour of 6-12 vol.% flyash reinforced A356 composite under different loads (10 - 80 N) while maintaining a constant sliding speed of 1 m/s. Wear graphs were obtained by employing the weight loss method. Under low load condition below 20 N, wear rate of the A356-(6-12 vol.%) flyash reinforced composite was very much similar compared to unreinforced alloy. However, as applied load increased above 20 N, wear rate escalated due to curling effects. Notably, as vol.% of the reinforcement increased, significant reduction in wear rate was observed[30]. According to Prabhudev et al.[31], the addition of 0.5 wt.% copper reinforcement led to a considerable enhancement in the wear-related characteristics in A356 alloy. The researchers noted that the oxide layer which may have formed between the mating surfaces and the friction force increased with application of normal pressure and sliding distance. Further, Kori et al.[32] reported that adding small amounts of alloying element magnesium (0.3-1 wt.%) to A356 alloy altered the acicular eutectic silicon to a lamellar and fibrous structure, while α-Al remained unmodified.

Overall, various reinforcement addition to the matrix A356 have led to improvements in its wear properties, making it more suitable for demanding industrial applications. The novelty of the work is incorporation of low melting copper coated zinc particles as reinforcements in A356 matrix alloy and investigate the change in microstructure, hardness, and wear properties of A356 alloy with trace addition of copper and zinc reinforcements coated with copper.

2. Experimental

Present study used a two-step stir casting method to prepare experimental composites using A356+1wt.% Mg as the matrix (alloy A) and trace addition of copper and zinc as reinforcements. To retain zinc as a separate identity in composite (melting point of zinc- 480°C), copper coating with a coating thickness of 10-12 µm was done on zinc particles using electrolytic copper coating method. A small amount of alkaline powder was added into the melt to avoid formation of slag and solid hexafluroethane as degasifying agent. Reinforcements were added into Al matrix with constant stirring at 150 RPM for 10 min so that the reinforcements dispersed uniformly in the matrix[33]. Figure 1 shows the fabricated as-cast composites bar and individual samples used for characterization. Table 1 shows the designations of the fabricated composites.

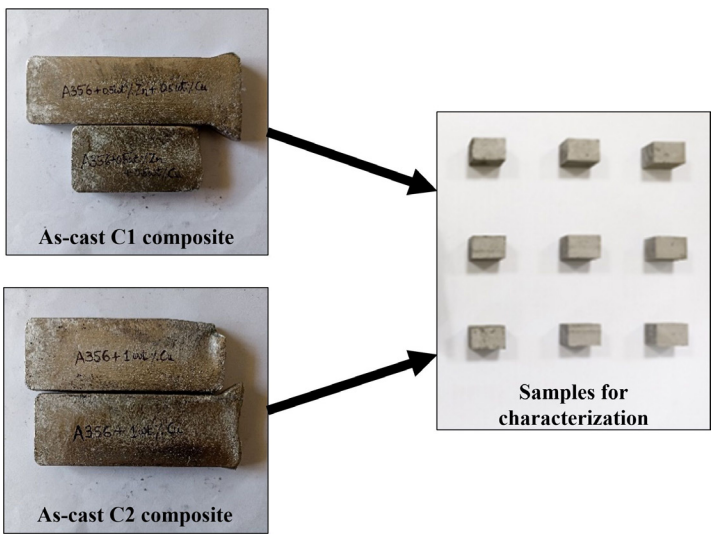

Figure 1. Fabricated composites.

Table 1. Fabricated composites with its designations.

Alloy Composition	A	C1	C2
Magnesium (wt.%)	1	1	1
Copper (wt.%)	0	0.5	1
Zinc (wt.%)	0	0.5	0

The composites were subjected to peak aging conditions by solutionizing at 520°C for 2 h, followed by water quenching at 60°C and aging at 100 and 200°C separately at different intervals of time. The peak aged samples and their micro-Vickers hardness was evaluated using ASTM E384 standards with the load of 200 gmf and dwell time of 15 sec to determine the peak hardness value[33]. Scanning Electron Microscope (SEM) images were used for microstructural analysis of composites and the distribution of reinforcement material was verified using Energy Dispersive X-ray analysis (EDAX). Cubic specimens are taken from multiple locations of the cast components to analyse the dispersion of Cu and Cu coated Zn particles. The specimens are meticulously polished, buffed, and etched with Keller's reagent, which contains 95 ml of water, 2.5 ml of nitric acid, 1.5 ml of hydrochloric acid, and 1.0 ml of hydrofluoric acid. This etching method enhances the visibility of reinforcements within the matrix. Wear tests were performed using an ASTM G99-04 by using Pin-On-Disc wear testing equipment. Before the wear tests, cylindrical pins of matrix alloy and composites were prepared using a wire EDM process and used as test specimen. Figure 2 displays the wear pin specimens of alloy A, C1 and C2 composites (ϕ10 mm) used to conduct wear test. Throughout the experiment, applied load was varied from 20-60 N maintaining constant sliding speed of 1 m/s and sliding distance of 3000 m. The equipment measured the wear and frictional force simultaneously at a track radius of 60 mm. The surface roughness of pin sample and track disc was noted to be 0.81 and 0.4 µm respectively. In order to validate the system generated wear (µm) results, mass loss was measured for each test sample at regular sliding distance interval of 500 m and wear rate (mm^3/m) was calculated. The wear rate was calculated manually using Equation 1 and coefficient of friction (COF) was system generated in steady state period.

$$Wr = \frac{\Delta m}{\rho * S} \tag{1}$$

$$\Delta m = m1 - m2$$

$$S = \frac{\pi * D * N * 60}{1000}$$

where, Wr is the wear rate (mm^3/m)
Δm is the mass loss (mg), m1- Initial weight (mg), m2- Final weight (mg),
ρ is the density of material
S is the sliding distance (m), D is the track diameter (mm),
The Pin-On-Disc tribometer used in the present study is shown in Figure 3.

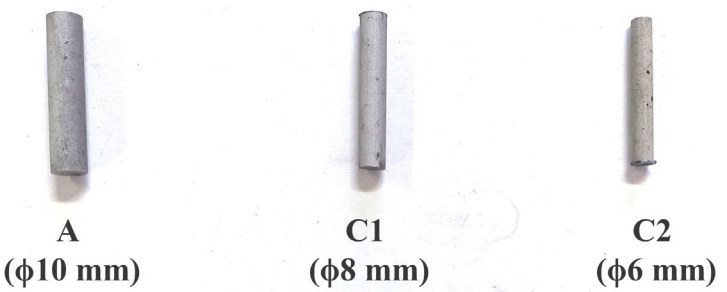

Figure 2. As-cast pin specimens used for wear test.

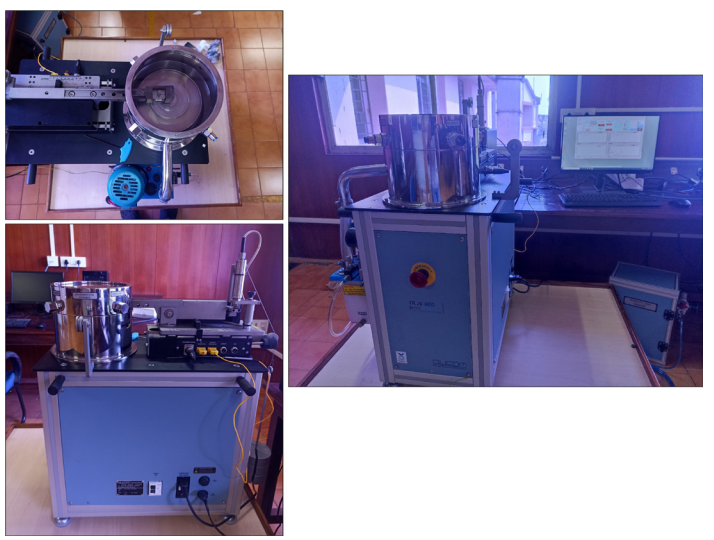

Figure 3. Pin-On-Disc tribometer.

3. Results and Discussion

3.1. Microstructure analysis

Before the microstructure study, samples were polished and etched for 25 sec using Keller's reagent and then examined using SEM microscopy along with EDS analysis[34]. Matrix alloy A showed the presence of pro-eutectic aluminum phase well-dispersed along the fine eutectic colonies of Al-Si. The grain size observed was comparatively large and the eutectic colony appeared coarse. This could possibly be attributed to insufficient alloying elements that are typically responsible for regulating grain size. The α-Al phase exhibited a dendritic structure, which was attributed to multiple eutectic reactions and the presence of certain alloying elements that have the ability to dissolve in aluminum.

To ensure that zinc particles remained separate and identifiable within a composite material, an electrolytic method was used to coat them with copper. The resulting copper coating had a thickness of 10-12 µm, and the existence of a Cu coating on the zinc particles was confirmed by Energy Dispersive X-ray analysis (EDAX) done at multiple locations. Figure 4 depicts the EDAX results confirming copper coating on zinc particles. This was necessary to prevent the zinc from melting and maintain its distinctiveness within the composite.

The uniformity of the reinforcements in the C1 and C2 composites is shown in Figure 5. Copper-coated zinc reinforcement is clearly visible in Figure 6a, while Figure 6b shows copper reinforcement in a random location. As seen in Figure 5, C1 composite has an intermediate grain size structure, whereas the C2 composite has a highly fine grain structure. This was attributed to the significant temperature difference between copper and matrix A occurred during synthesis process. Figure 7 depicts the EDAX results confirming the presence of Cu coated Zn in C1 composite and Cu in C2 composite.

3.2. Hardness measurement

In as-cast condition, C1 and C2 composites exhibited a significant increase in Vickers Hardness Number (VHN) compared to the matrix A. Specifically, the VHN of matrix A was measured at 54, whereas the VHN values for C1 and C2 composites containing 0.5 and 1 wt.% of Cu reinforcement were 69 and 85 respectively and are presented in Figure 8. This significant improvement of hardness value in C2 composite can primarily be attributed to the presence of hard copper dispersoids with matrix, which have positive effect on overall hardness improvement of the composite. Due to smaller volume expansion of added reinforcement, the matrix undergoes plastic deformation to accommodate reinforcement particles[35]. This lead to a higher density of dislocations, which increased resistance to plastic deformation thereby contributing effectively in overall hardness improvement in C1 and C2 composites.

Figure 9 illustrates the peak hardness value of heat treated C1 and C2 composite compared with matrix alloy A. Compared to as-cast matrix A, age hardening of the composites resulted in significant improvements in hardness, with 105-121% and 52-69% increase observed during 100 and 200°C aging respectively. The reason for significant improvement in hardness results were due to precipitation of solute-rich phases from the supersaturated solid solution during aging[36]. From hardness test, it was noticed that the hardness values were higher for samples aged at lower temperature (100°C) compared to those aged at higher temperature (200°C). Nevertheless, time taken to reach the maximum hardness level was longer at 100°C, which might be attributed to the aging kinetics. The formation of metastable strengthening phase which are finely dispersed along the matrix, during aging process contributed to hardness improvement in peak aged samples. Additionally, samples aged at 100°C resulted in formation of a greater number of fine precipitates than samples aged at 200°C. The results also suggest that the inclusion of 1 wt.% Cu reinforcement enhanced both the rate and effectiveness of age hardening. With an increase in the wt.% of Cu, a greater number of intermetallics were formed, which in turn led to a significant hardness improvement. Furthermore, the addition of 1 wt.% magnesium to A356 resulted in solid solution strengthening by the formation of Mg_2Si intermetallics.

3.3. Wear behaviour

Tables 2 to 4 shows the wear results obtained using mass loss method (wear rate in mm^3/m) and system generated wear (µm). Figures 10 to 12 depicts the system generated wear behaviour of matrix A, C1 and C2 composites under different applied loads. The wear behavior trend of the system generated wear (µm) and wear rate (mm^3/m) determined through the mass loss method are observed to be consistent.

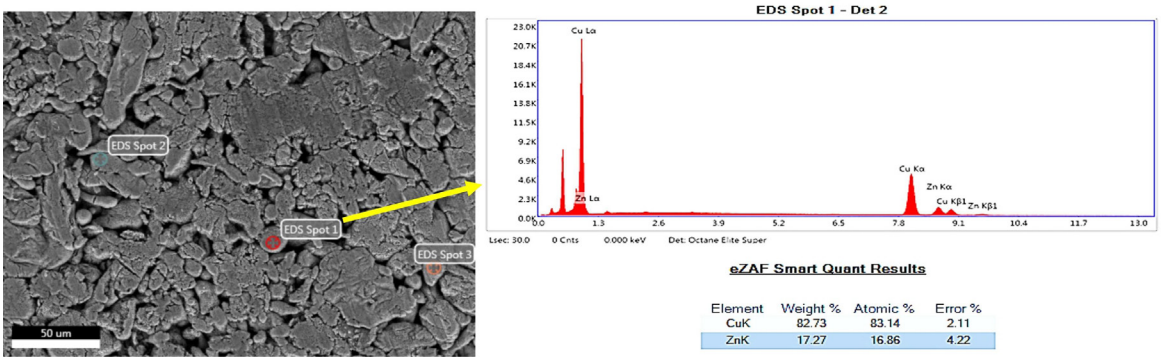

Figure 4. EDAX results confirming copper coating.

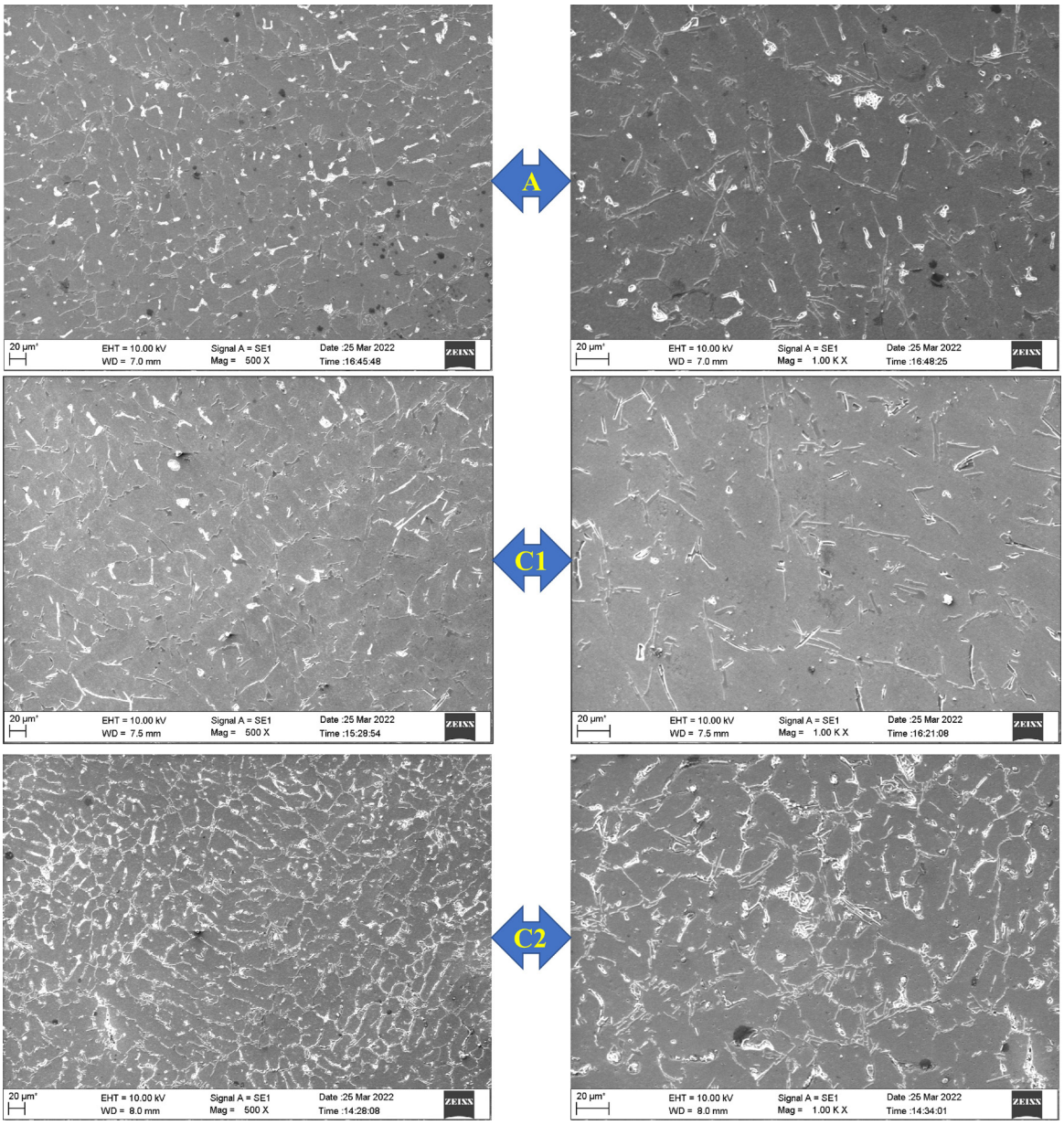

Figure 5. SEM images of as-cast matrix A, C1 and C2 composite.

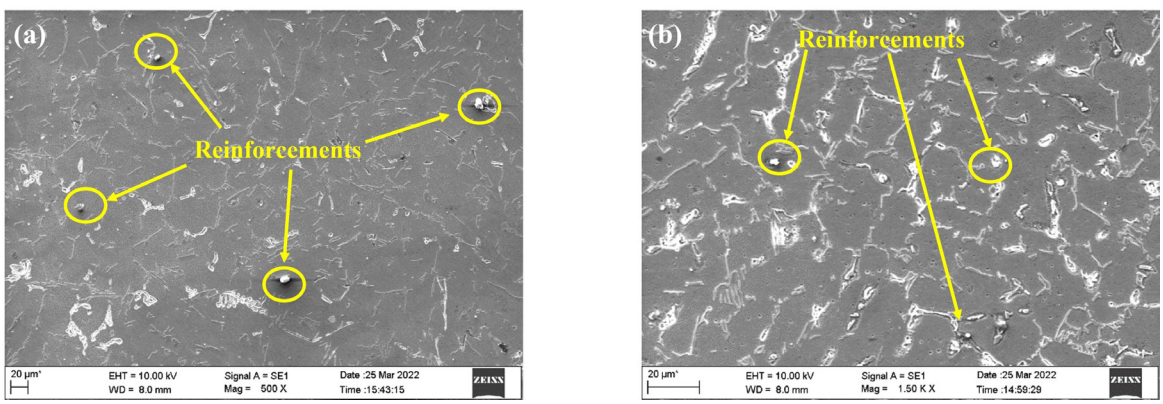

Figure 6. Reinforcement distribution of (a) C1 and (b) C2 composites.

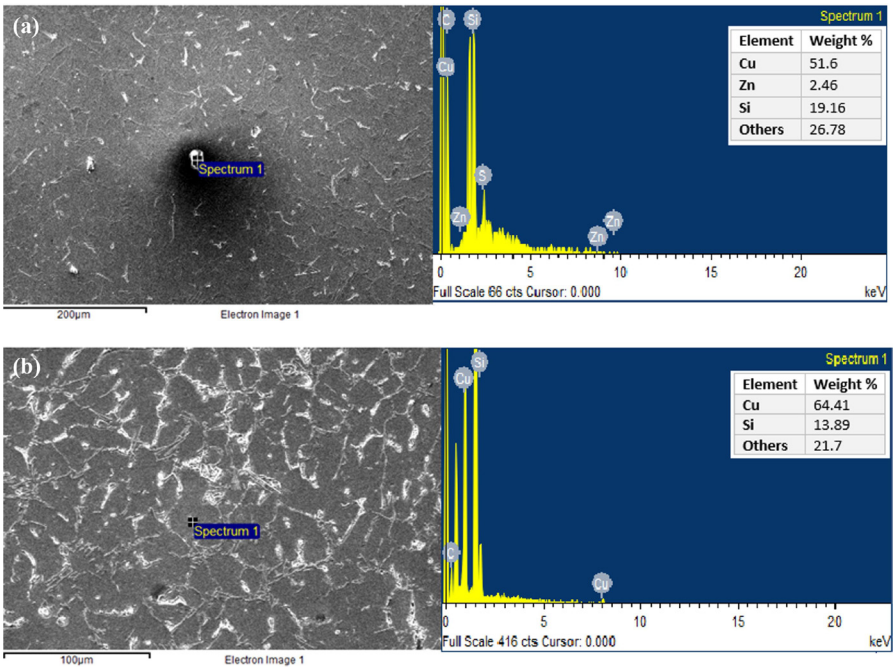

Figure 7. EDAX report showing the presence of (a) Cu coated Zn in C1 composite and (b) Cu in C2 composite.

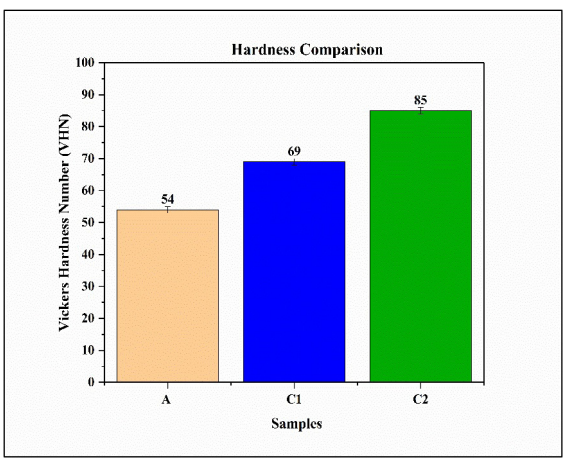

Figure 8. Vickers hardness result.

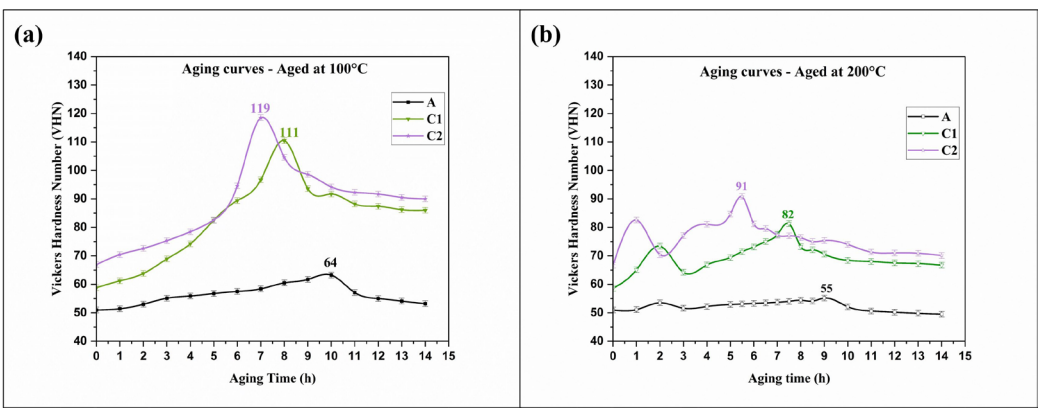

Figure 9. Aging curve of composites compared with matrix alloy A aged at (a) 100°C (b) 200°C.

Table 2. Wear results obtained for alloy A.

Load (N)	Sliding Distance (m)	Mass loss method							System generated		
		Mass loss Δm (m1-m2) (mg)			Speed (RPM)	Wear rate W_r (10^{-5} mm^3/m)			Wear (μm)		
		A (as-cast)	A (aged at 100°C)	A (aged at 200°C)		A (as-cast)	A (aged at 100°C)	A (aged at 200°C)	A (as-cast)	A (aged at 100°C)	A (aged at 200°C)
20	500	0.8	0.6	0.7	200	0.42	0.32	0.37	54	38	47
20	1000	1.9	1.6	1.8	200	0.50	0.42	0.48	75	54	62
20	1500	3.1	3.6	4.1	200	0.55	0.64	0.72	104	85	93
20	2000	4.5	7	7.8	200	0.60	0.93	1.03	146	124	132
20	2500	6.4	9.9	11.6	200	0.68	1.05	1.23	173	141	159
20	3000	8.2	14.1	15.9	200	0.72	1.25	1.40	204	166	187
40	500	2.4	1.8	2.1	200	1.27	0.95	1.11	83	62	74
40	1000	7.5	6.3	6.8	200	1.99	1.67	1.80	132	111	121
40	1500	17.2	14.4	15.7	200	3.04	2.54	2.77	197	167	185
40	2000	33.1	26.9	29.1	200	4.39	3.57	3.86	286	232	256
40	2500	53.9	46.8	48.9	200	5.72	4.96	5.19	374	330	342
40	3000	78	70.4	72.6	200	6.89	6.22	6.42	454	408	421
60	500	5.4	4.1	4.9	200	2.86	2.17	2.60	127	101	119
60	1000	13.9	11.1	12.7	200	3.68	2.94	3.37	161	130	147
60	1500	32.2	25	27.3	200	5.69	4.42	4.82	249	194	210
60	2000	52.2	43.3	48.4	200	6.92	5.74	6.42	302	252	281
60	2500	85.5	74.5	82.1	200	9.07	7.90	8.71	398	344	376
60	3000	123.6	113.4	118.7	200	10.92	10.02	10.49	476	432	455

Table 3. Wear results obtained for C1 composite.

Load (N)	Sliding Distance (m)	Mass loss method							System generated		
		Mass loss Δm (m1-m2) (mg)			Speed (RPM)	Wear rate W_r (10^{-5} mm^3/m)			Wear (μm)		
		A (as-cast)	A (aged at 100°C)	A (aged at 200°C)		A (as-cast)	A (aged at 100°C)	A (aged at 200°C)	A (as-cast)	A (aged at 100°C)	A (aged at 200°C)
20	500	0.7	0.5	0.6	200	0.38	0.27	0.32	45	32	36
20	1000	1.7	1.1	1.2	200	0.46	0.30	0.32	58	38	41
20	1500	3.3	2.3	2.8	200	0.59	0.41	0.50	76	54	66
20	2000	6.4	5.1	5.8	200	0.86	0.68	0.78	111	86	102
20	2500	9.1	7.3	8.7	200	0.98	0.78	0.93	128	102	121
20	3000	12.5	9.6	11.9	200	1.12	0.86	1.07	145	110	138
40	500	1.9	1.2	1.5	200	1.02	0.64	0.81	64	42	54
40	1000	4.9	3.5	4.3	200	1.32	0.94	1.15	85	61	75
40	1500	10.6	6.9	8.2	200	1.90	1.24	1.47	123	80	98
40	2000	19.9	12.8	16.4	200	2.67	1.72	2.20	174	110	144
40	2500	36.7	22.5	30.2	200	3.94	2.42	3.24	255	157	210
40	3000	53.2	31.7	45.8	200	4.76	2.84	4.10	310	184	265
60	500	3.7	2.2	2.8	200	1.99	1.18	1.50	86	51	65
60	1000	13	6.4	8.8	200	3.49	1.72	2.36	152	76	102
60	1500	26.8	15.6	20.6	200	4.80	2.79	3.69	207	121	162
60	2000	43.5	26.4	35.5	200	5.84	3.55	4.77	252	154	206
60	2500	67.4	38.3	52.7	200	7.24	4.11	5.66	313	180	244
60	3000	91.8	53.7	73.8	200	8.22	4.81	6.61	354	208	286

Table 4. Wear results obtained for C2 composite.

Load (N)	Sliding Distance (m)	Mass loss method							System generated		
		Mass loss Δm (m1-m2) (mg)			Speed (RPM)	Wear rate W_r (10^{-5} mm^3/m)			Wear (µm)		
		A (as-cast)	A (aged at 100°C)	A (aged at 200°C)		A (as-cast)	A (aged at 100°C)	A (aged at 200°C)	A (as-cast)	A (aged at 100°C)	A (aged at 200°C)
20	500	0.5	0.3	0.4	200	0.27	0.16	0.22	38	22	29
20	1000	1.3	0.9	1	200	0.35	0.24	0.27	47	32	37
20	1500	2.2	1.8	2.1	200	0.39	0.32	0.38	55	43	50
20	2000	4.1	3.2	3.5	200	0.55	0.43	0.47	74	57	63
20	2500	7.1	5.8	6.4	200	0.76	0.62	0.69	99	82	89
20	3000	9.3	8.3	8.6	200	0.83	0.74	0.77	109	94	100
40	500	1.7	0.6	1.4	200	0.91	0.32	0.75	58	31	49
40	1000	4.1	3.2	3.6	200	1.10	0.86	0.97	71	56	63
40	1500	9.9	6.3	7.6	200	1.78	1.13	1.36	116	74	92
40	2000	18.1	11.5	15.1	200	2.43	1.55	2.03	158	102	130
40	2500	32.2	19.2	24.1	200	3.46	2.07	2.59	224	135	169
40	3000	49.2	28.5	41.3	200	4.41	2.56	3.70	287	166	241
60	500	3.1	0.9	2.1	200	1.67	0.48	1.13	72	22	51
60	1000	11.2	4.6	7.5	200	3.01	1.24	2.02	131	52	86
60	1500	24.3	11.9	18.9	200	4.36	2.13	3.39	189	96	147
60	2000	38.6	20.8	32.3	200	5.19	2.80	4.34	226	121	188
60	2500	62.9	32.8	45.8	200	6.77	3.53	4.93	293	152	213
60	3000	78.6	48.5	59.5	200	7.05	4.35	5.33	305	188	229

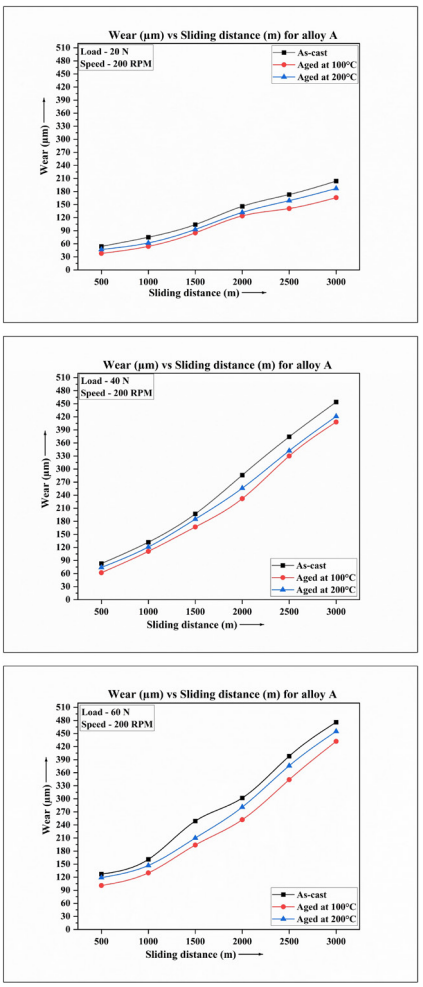

Figure 10. Wear rate vs. sliding distance for alloy A.

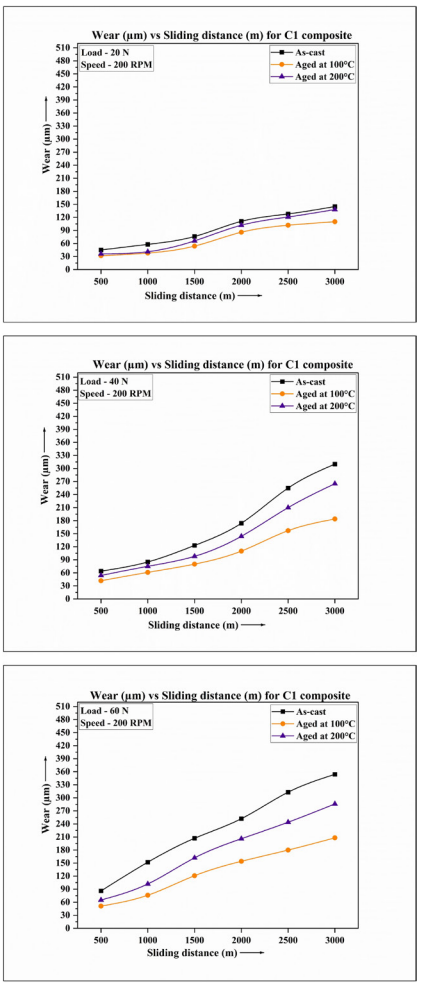

Figure 11. Wear rate vs. sliding distance for C1 composite.

Therefore further explanations are provided based on system generated wear graphs. From the graphs, it is clear that with increase in applied load, the wear of C1 and C2 composites increased. Under a low load condition of 20 N, wear behaviour of C1 and C2 composites was comparable. However, upon increasing applied load to 40 N, maximum wear experienced by the composites was significantly reduced. However, when load was further increased to 60 N, wear of composites increased slightly due to increased plastic deformation, which increased the probability of subsurface cracking and significant material loss[37,38].

A higher hardness value in C1 and C2 composites indicates a higher resistance to plastic deformation and material removal during sliding contact, which can result in reduced wear. Increasing the hardness of A356 alloy through heat treatment and addition of reinforcing particles, resulted in enhanced wear resistance in C1 and C2 composites. The harder the material, the better it can resist wear and withstand the abrasive and adhesive forces encountered during sliding contact with a counterbody[9].

In terms of wear resistance, the C2 composite exhibited superior performance than the C1 composite at high load condition attributed by the presence of copper reinforcements and hardness improvement thus preventing delamination and hence material loss. The inclusion of 1 wt.% Cu reinforcement into matrix A enhanced the effective contact between the asperities and the opposing surface, leading to reduced wear in the C2 composite[39].

Age hardening treatment also contributed to improved wear resistance in C1 and C2 composites. Compared to higher temperatures (200°C), lower aging temperatures (100°C) had a more significant effect on improving wear resistance. Lower aging temperature (100°C) resulted in the generation of a larger number of intermediate phases with a smaller average interparticle distance, which in turn increased the number of finer intermetallics. This contributed to an increase in matrix coherency strain, ultimately leading to higher wear resistance. Overall, 100°C peak aged C2 composite exhibited highest wear resistance among the composites and unreinforced alloy A. These findings are consistent with results reported by previous researchers[31,40-42]. Generally, the hardness of both the matrix and the reinforcement and the density of the intermetallics formed, are directly proportional to wear resistance[43]. Thus, increasing the hardness through heat treatment can improve the abrasion wear resistance[11].

There are several factors that can influence the friction coefficient of a worn surface, including sliding distance, load, and temperature[44]. Figures 13 and 14 present the friction coefficient curves of C1 and C2 composites at varying loads and sliding distances. Figures 13 and 14 illustrate that coefficient of friction (COF) in C1 and C2 composites increased with increasing sliding distance, under studied conditions.

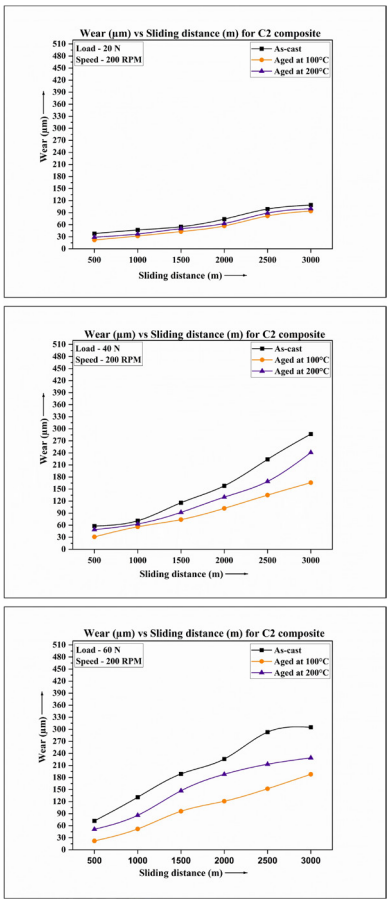

Figure 12. Wear rate vs. sliding distance for C2 composite.

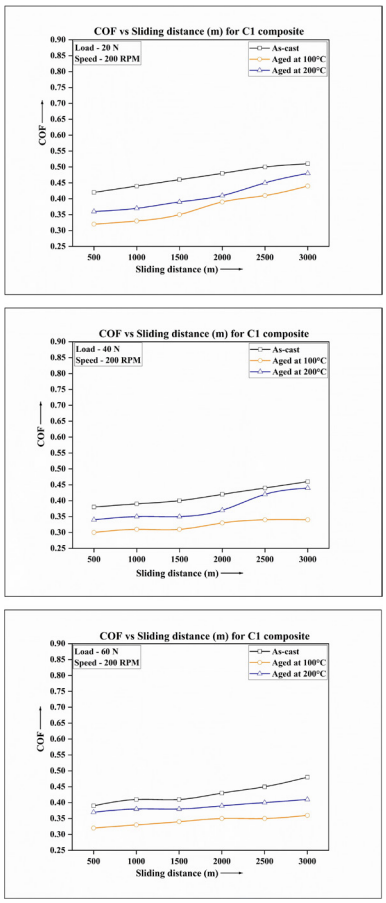

Figure 13. COF vs. sliding distance for C1 composite.

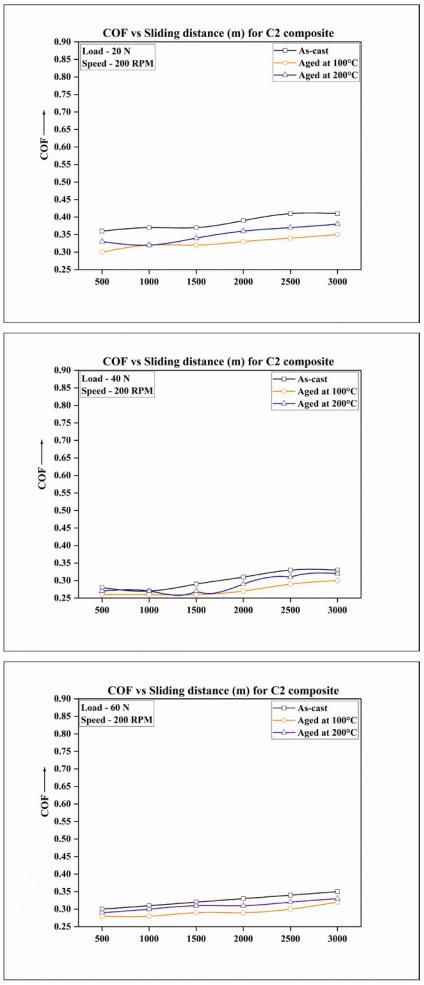

Figure 14. COF vs. sliding distance for C2 composite.

This was attributed to rise in temperature due to increased friction force between the contact surfaces during sliding action. At an applied load of 20 N, as-cast C2 composite displayed a lower average COF compared to C1 composite, due to the formation of a mechanically mixed layer (MML) that generated a smooth surface, reducing friction. With increased applied load to 40 N, the average COF decreased for both composites, with C2 composite displaying a lower COF compared to C1. However, at applied load of 60 N, COF marginally increased in composites, possibly due to disruption of the MML and wear debris generated between the pin sample and the disc. On compared to as-cast composites C1 and C2, 100 and 200°C peak aged samples showed lower COF values in the studied condition. High COF was observed in as-cast C1 and C2 composites due to the softness and lower hardness value of composites when compared to peak aged samples. Peak aged samples resulted in higher hardness values resulting in more resistance to plastic deformation and lesser frictional force.

The worn surfaces of as-cast C1, C2 composites were analysed using SEM and the results are presented in Figure 15. The SEM analysis indicated that as-cast C1 composite had a higher degree of fracture compared to the C2 composite.

The worn surface of as-cast C1 composite showed both continuous and discontinuous grooves across the surface, indicating mild abrasive wear at lower load of 20 N. With increasing load, abrasive and delaminating wear became more predominant causing severe wear at higher loads. In contrast, at lower load of 20 N, the worn surface of C2 composite showed furrows and spalling pits, with minimal wear mainly caused by adhesive and mild fatigue wear. As the applied load was increased above 40 N, wear intensified and a combination of abrasive and severe adhesive wear was observed. This resulted in numerous pits, flakes, and internal cracks due to delamination wear caused by shear forces and frictional heat[45,46].

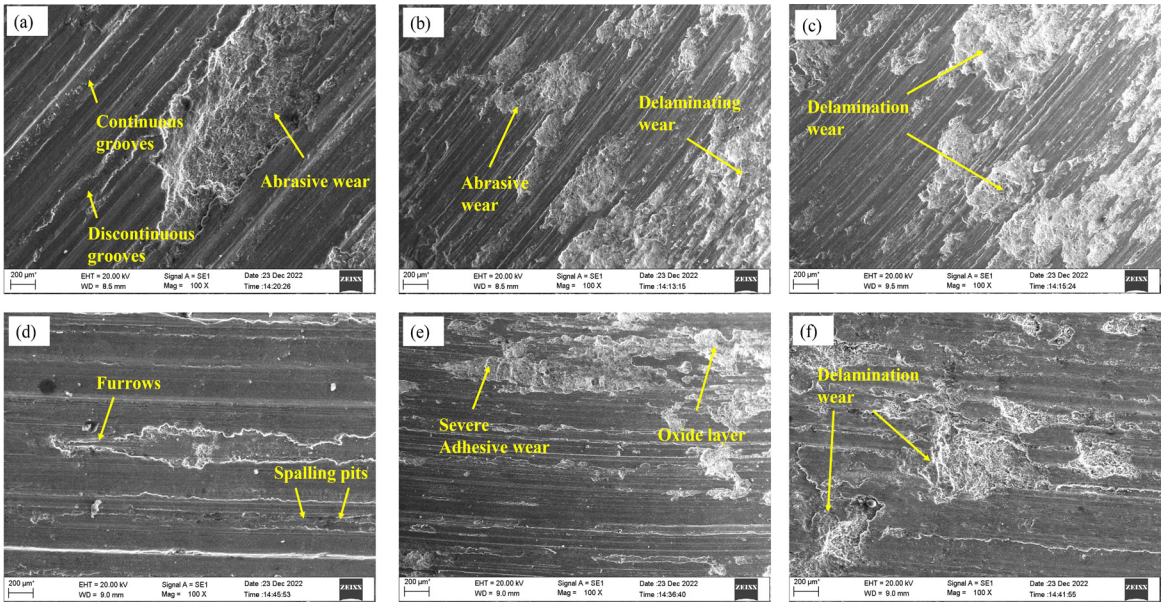

Figure 15. Worn surfaces of C1 composite (a)~(c) (a) 20 N, (b) 40 N, (c) 60 N. Worn surfaces of C2 composite (d) ~(f): (d) 20 N, (e) 40 N, (f) 60 N.

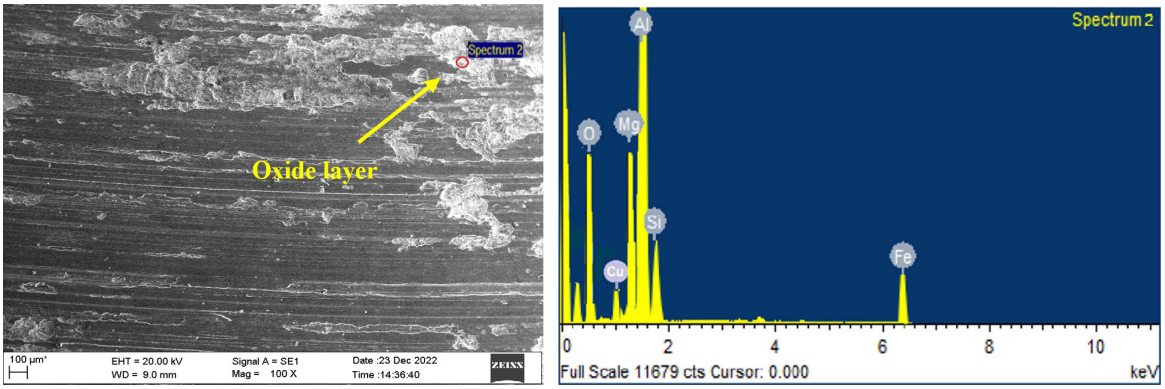

Figure 16. EDAX results of C2 composite at applied load of 40 N.

At lower load conditions, the worn surface of the composites showed fine parallel abrasive grooves and an oxide layer, indicating mild abrasive wear and oxidative wear as primary wear mechanisms. Oxide layer was formed by the Fe-rich phases present in the counter disc material, acting as a lubricant and reducing the wear rate. At higher load conditions (40-60 N), formation of the Fe-rich oxide layer was confirmed by EDAX analysis, leading to an improvement in wear resistance. Figure 16 shows EDAX results of C2 surface, confirming the presence of the Fe-rich oxide layer.

4. Conclusions

1. Through a two-step stir casting process, copper-coated zinc particles were effectively used to reinforce the A356 alloy. This study demonstrated the feasibility of incorporating a reinforcement material with a lower melting point (zinc) into a matrix with a higher melting point matrix to produce an A356 alloy composite.
2. The inclusion of copper to A356 facilitated age hardening under both as-quenched and aging. 0.5 wt.% copper-reinforced composite aged at 100°C, exhibited 105% increase in hardness, although the duration of the process was longer. In contrast, 1 wt.% copper-reinforced composite achieved peak hardness of 119 VHN (121% improvement over the as-cast matrix A) in a shorter time.
3. Under lower load conditions (20 N), C1 composite (reinforced with 0.5 wt.% Zn+0.5 wt.% Cu) displayed 85-97% and 48-83% enhancement in wear resistance when peak aged at 100 and 200°C respectively. Meanwhile, C2 alloy (reinforced with 1 wt.% Cu) exhibited a 117-134% and 102-104% increase in wear resistance when peak aged at 100 and 200°C respectively.
4. Under higher load conditions (40-60 N), C1 composites showed 112-128% and 58-66% improvement in wear resistance when peak aged at 100 and 200°C respectively. Meanwhile, C2 composite (reinforced with 1 wt.% Cu) exhibited 153-210% and 87-108% increase in wear resistance when peak aged at 100 and 200°C respectively.

5. References

1. Shanmughasundaram P, Subramanian R, Prabhu G. Some studies on aluminium -fly ash composites fabricated by two step stir casting method. Eur J Sci Res. 2011;63(2):204-18.
2. Chak V, Chattopadhyay H, Dora TL. A review on fabrication methods, reinforcements and mechanical properties of aluminum matrix composites. J Manuf Process. 2020;56(May):1059-74. http://dx.doi.org/10.1016/j.jmapro.2020.05.042.
3. Kala H, Mer KKS, Kumar S. A review on mechanical and tribological behaviors of stir cast aluminum matrix composites. Procedia Mater. Sci. 2014;6(1):1951-60. http://dx.doi.org/10.1016/j.mspro.2014.07.229.
4. James J, Raja Annamalai A. Tribological behaviour and wear fashion of processed AA6061/ZrO_2 composite. Ind Lubr Tribol. 2018;70(9):1815-24. http://dx.doi.org/10.1108/ILT-12-2017-0382.
5. Toor ZS, Zafar MM. Corrosion degradation of aluminium alloys using a computational framework. Tribol. Mater. 2022;1(4):150-6. http://dx.doi.org/10.46793/tribomat.2022.019.
6. Sarkar AD. Wear of aluminium-silicon alloys. Wear. 1975;31(2):331-43. http://dx.doi.org/10.1016/0043-1648(75)90167-2.
7. Clarke J, Sarkar AD. Wear characteristics of as-cast binary aluminium-silicon alloys. Wear. 1979;54(1):7-16. http://dx.doi.org/10.1016/0043-1648(79)90044-9.
8. Li YJ, Brusethaug S, Olsen A. Influence of Cu on the mechanical properties and precipitation behavior of AlSi7Mg0. 5 alloy during aging treatment. Scr Mater. 2006;54(1):99-103. http://dx.doi.org/10.1016/j.scriptamat.2005.08.044.
9. Torabian H, Pathak JP, Tiwari SN. Wear characteristics of Al-Si alloys. Wear. 1994;172(1):49-58. http://dx.doi.org/10.1016/0043-1648(94)90298-4.
10. Vencl A, Bobić I, Stanković M, Hvizdoš P, Bobić B, Stojanović B, et al. Influence of secondary phases in A356 MMCs on their mechanical properties at macro and nanoscale. J Braz Soc Mech Sci Eng. 2020;42(3):115. http://dx.doi.org/10.1007/s40430-020-2197-6.
11. Vencl A, Bobić I, Mišković Z. Effect of thixocasting and heat treatment on the tribological properties of hypoeutectic Al–Si alloy. Wear. 2008;264(7-8):616-23. http://dx.doi.org/10.1016/j.wear.2007.05.011.
12. Davis J. Alloying: understanding the basics. ASM Int. 2001;4(1):351-416. http://dx.doi.org/10.1136/oem.42.11.746.
13. Stojanović B, Tomović R, Gajević S, Petrović J, Miladinović S. Tribological behavior of aluminum composites using Taguchi. Adavanced Eng. Lett. 2022;1(1):28-34. http://dx.doi.org/10.46793/adeletters.2022.1.1.5.

14. Vencl A, Vučetić F, Bobić B, Pitel J, Bobić I. Tribological characterisation in dry sliding conditions of compocasted hybrid A356/SiCp /Grp composites with graphite macroparticles. Int J Adv Manuf Technol. 2019;100(9-12):2135-46. http://dx.doi.org/10.1007/s00170-018-2866-0.
15. Zeren M, Karakulak E, Gümüş S. Influence of Cu addition on microstructure and hardness of near-eutectic Al-Si-xCu-alloys. Trans Nonferrous Met Soc China. 2011;21(8):1698-702. http://dx.doi.org/10.1016/S1003-6326(11)60917-5.
16. Shivaprasad CG, Aithal K, Narendranath S, Desai V, Mukunda PG. Effects of 4.5% copper addition and melt treatment on microstructure and wear properties of Al-7Si alloy. Appl Mech Mater. 2015;766-767:410-5. http://dx.doi.org/10.4028/www.scientific.net/AMM.766-767.410.
17. Chee CY, Azmi A. Preparation and characterization of copper/copper coated silicon carbide composites. Int J Precis Eng Manuf. 2014;15(6):1215-21. http://dx.doi.org/10.1007/s12541-014-0459-x.
18. Beigi Khosroshahi N, Taherzadeh Mousavian R, Azari Khosroshahi R, Brabazon D. Mechanical properties of rolled A356 based composites reinforced by Cu-coated bimodal ceramic particles. Mater Des. 2015;83:678-88. http://dx.doi.org/10.1016/j.matdes.2015.06.027.
19. Shukla S, Seal S, Rahaman Z, Scammon K. Electroless copper coating of cenospheres using silver nitrate activator. Mater Lett. 2002;57(1):151-6. http://dx.doi.org/10.1016/S0167-577X(02)00722-X.
20. Anyalebechi PN. Analysis of the effects of alloying elements on hydrogen solubility in liquid aluminum alloys. Scr Metall Mater. 1995;33(8):1209-16. http://dx.doi.org/10.1016/0956-716X(95)00373-4.
21. Vencl A, Bobic I, Stojanovic B. Tribological properties of A356 Al-Si alloy composites under dry sliding conditions. Ind Lubr Tribol. 2014;66(1):66-74. http://dx.doi.org/10.1108/ILT-06-2011-0047.
22. Prasad BK, Venkateswarlu K, Modi OP, Jha AK, Das S, Dasgupta R, et al. Sliding wear behavior of some Al-Si Alloys: role of shape and size of Si particles and test conditions. Metall Mater Trans, A Phys Metall Mater Sci. 1998;29(11):2747-52. http://dx.doi.org/10.1007/s11661-998-0315-7.
23. Stojanović B, Gajević S, Kostić N, Miladinović S, Vencl A. Optimization of parameters that affect wear of A356/Al_2O_3 nanocomposites using RSM, ANN, GA and PSO methods. Ind Lubr Tribol. 2022;74(3):350-9. http://dx.doi.org/10.1108/ILT-07-2021-0262.
24. Zhu M, Jian Z, Yang G, Zhou Y. Effects of T6 heat treatment on the microstructure, tensile properties, and fracture behavior of the modified A356 alloys. Mater Des. 2012;36:243-9. http://dx.doi.org/10.1016/j.matdes.2011.11.018.
25. Imurai S, Kajornchaiyakul J, Thanachayanont C. Age hardening and precipitation behavior of an experimental cast Al-Mg-Si alloy treated by T6 and T6I6 heat treatments. Warasan Khana Witthayasat Maha Witthayalai Chiang Mai. 2010;37(2):269-81.
26. Vencl A, Bobic I, Arostegui S, Bobic B, Marinković A, Babić M. Structural, mechanical and tribological properties of A356 aluminium alloy reinforced with Al_2O_3, SiC and SiC+ graphite particles. J Alloys Compd. 2010;506(2):631-9. http://dx.doi.org/10.1016/j.jallcom.2010.07.028.
27. Bobić I, Ružić J, Bobić B, Babić M, Vencl A, Mitrović S. Microstructural characterization and artificial aging of compo-casted hybrid A356 / SiCp / Grp composites with graphite macroparticles. Mater Sci Eng A. 2014;612(1):7-15. http://dx.doi.org/10.1016/j.msea.2014.06.028.
28. Hassan AM, Alrashdan A, Hayajneh MT, Mayyas AT. Wear behavior of Al-Mg-Cu-based composites containing SiC particles. Tribol Int. 2009;42(8):1230-8. http://dx.doi.org/10.1016/j.triboint.2009.04.030.
29. Alias TY, Haque MM. Wear properties of aluminum – silicon eutectic alloy. Int Conf Mech Eng. 2003;3(2):26-8.
30. Sudarshan, Surappa MK. Dry sliding wear of fly ash particle reinforced A356 Al composites. Wear. 2008;265(3-4):349-60. http://dx.doi.org/10.1016/j.wear.2007.11.009.
31. Prabhudev MS, Auradi V, Venkateswarlu K, Siddalingswamy NH, Kori SA. Influence of Cu addition on dry sliding wear behaviour of A356 alloy. Procedia Eng. 2014;97:1361-7. http://dx.doi.org/10.1016/j.proeng.2014.12.417.
32. Kori SA, Prabhudev MS, Chandrashekharaiah TM. Studies on the microstructure and mechanical properties of A356 alloy with minor additions of copper and magnesium. Trans Indian Inst Met. 2009;62(4–5):353-6. http://dx.doi.org/10.1007/s12666-009-0052-7.
33. Nithesh K, Nayak R, Hande R, Sharma S, Gowri Shankar MC, Doddapaneni S. Dual role of trace elements in magnesium dissolved age hardened A356 alloy on microstructure and peak micro hardness. Manuf Rev (Les Ulis). 2023;10(5):5. http://dx.doi.org/10.1051/mfreview/2023003.
34. Kashimat N, Sharma S, Nayak R, Manjunathaiah KB, Shettar M, Chennegowda GM. Experimental investigation of mechanical property and wear behaviour of T6 treated A356 alloy with minor addition of copper and zinc. J. Compos. Sci. 2023;7(4):149. http://dx.doi.org/10.3390/jcs7040149.
35. Doddapaneni S, Kumar S, Shettar M, Rao S, Sharma S, MC G. Experimental investigation to confirm the presence of TiB2 reinforcements in the matrix and effect of artificial aging on hardness and tensile properties of stir-cast LM4-TiB2 composite. Crystals (Basel). 2022;12(8):1114. http://dx.doi.org/10.3390/cryst12081114.
36. Rajan TV, Sharma CP, Ashok S. Heat treatment: principles and techniques. New Delhi: PHI Learning Private Limited; 2011. (vol. 2).
37. Shankar G, Sharma SS, Kini A, Jayashree PK, Gurumurthy BM. Study of wear behavior and mechanical mixed layer on artificial aged Al6061 composite reinforced with B4C particles. Indian J Sci Technol. 2016;9(12):88073. http://dx.doi.org/10.17485/ijst/2016/v9i12/88073.
38. Uthayakumar M, Kumaran ST, Aravindan S. Dry sliding friction and wear studies of fly ash reinforced AA-6351 metal matrix composites. Adv Tribol. 2013;2013:365602. http://dx.doi.org/10.1155/2013/365602.
39. Umanath K, Palanikumar K, Selvamani ST. Analysis of dry sliding wear behaviour of Al6061/SiC/Al_2O_3 hybrid metal matrix composites. Compos, Part B Eng. 2013;53:159-68. http://dx.doi.org/10.1016/j.compositesb.2013.04.051.
40. Kori SA, Prabhudev MS. Sliding wear characteristics of Al-7Si-0.3Mg alloy with minor additions of copper at elevated temperature. Wear. 2011;271(5-6):680-8. http://dx.doi.org/10.1016/j.wear.2010.12.080.
41. Palta A, Sun Y, Ahlatci H. Effect of copper addition on wear and corrosion behaviours of Mg_2Si particle reinforced composites. Mater Des. 2012;36:451-8. http://dx.doi.org/10.1016/j.matdes.2011.11.052.
42. Aigbodion VS, Hassan SB. Experimental correlations between wear rate and wear parameter of Al-Cu-Mg/bagasse ash particulate composite. Mater Des. 2010;31(4):2177-80. http://dx.doi.org/10.1016/j.matdes.2009.10.055.
43. Sawla S, Das S. Combined effect of reinforcement and heat treatment on the two body abrasive wear of aluminum alloy and aluminum particle composites. Wear. 2004;257(5-6):555-61. http://dx.doi.org/10.1016/j.wear.2004.02.001.
44. Zhao M, Wu G, Jiang L, Dou Z. Friction and wear properties of TiB_2/Al composite. Compos, Part A Appl Sci Manuf. 2006;37(11):1916-21. http://dx.doi.org/10.1016/j.compositesa.2005.12.018.
45. Prasad DS, Krishna AR. Tribological properties of A356.2/RHA composites. J Mater Sci Technol. 2012;28(4):367-72. http://dx.doi.org/10.1016/S1005-0302(12)60069-3.
46. Wu YC. Tailoring microstructure and its effect on wear behavior of an Al-7Si alloy reinforced with in situ formed Al_3Ti particulates. J Mater Res Technol. 2020;9(4):7136-48. http://dx.doi.org/10.1016/j.jmrt.2020.04.061.